Proceedings of the
Annual Stability Conference
Structural Stability Research Council
Atlanta, Georgia, April 21-24, 2026

Eigenvalue analysis of box girder cross-sections considering realistic bearing-type boundary conditions

T. G. Mythri[1], Pasupuleti N. Mohan[2], Aritra Chatterjee[3]

Abstract

Box girder sections used in viaduct structures to support high speed loading are susceptible to dynamic amplification and resonance due to moving loads. Dynamic analysis of these cross-sections is typically conducted using the modal superposition approach on a beam kinematic model. Eurocode BS EN 1991-2:2003 provides the only available guidance regarding such analysis and recommends consideration of torsional mode shapes in addition to flexure, if torsional frequencies are within less than 1.2 times the first natural frequency. There is a dearth of research supporting this recommendation. The methodology to include torsional and lateral mode shapes in beam vibration response is also unclear. Realistic boundary conditions for viaducts include bearing supports which provide compressional contact and partial moment restraint, whereas beam vibration solutions can accommodate simple supports and / or full torsional / flexural restraints only. To address these research gaps, this paper presents a solid finite element eigenvalue analysis of box girder viaducts with realistic boundary conditions. The results highlight the difference in natural frequencies and mode shapes between an analysis with perfect torsional restraint and another with realistic partial restraint. Existence of several cross-sectional distortional modes is observed. Finally, a moving load model that precludes the complexities of train-track interaction, while preserving the intricacies of cross-sectional deformation, reveals that although the beam model with idealized boundary conditions underpredicts torsional displacements, this does not significantly affect the total deflection of the girder. The findings are of potential significance towards stability analysis of box cross-sections under high speed moving loads.

1. Introduction

High speed railway (HSR), a potentially sustainable alternative to air travel, has expanded rapidly in the late twentieth and early twenty-first century, beginning with Shinkansen in Japan, followed by uptake in Europe and South Korea and explosive growth in China (UIC (International Union of Railways), 2023). HSR construction is ongoing in California, USA and in India where the first high speed railway line between Mumbai and Ahmedabad is being built, with significant countrywide expansion planned in the next decade.

[1] Postdoctoral Fellow, Michigan State University, <my3tumbalam@gmail.com>
[2] Doctoral Researcher, Indian Institute of Technology Kharagpur, <nagamohan.pasupulati@gmail.com>
[3] Assistant Professor, Indian Institute of Technology Kharagpur, <aritra@civil.iitkgp.ac.in>

Elevated viaducts are a common choice to support HSR lines, particularly in densely populated cities to ensure uninterrupted travel. The importance of dynamic effects in HSR viaduct design is universally acknowledged, requiring dynamic analysis at the design stage, which can be performed at varying degrees of complexity. The original solution for a bridge vibration problem was provided by Timoshenko (Timoshenko, 1922). Yang (Yang *et al.*, 1997) derived analytical solutions for moving loads on a beam including a speed parameter to predict resonance. This was later extended (Xu *et al.*, 2023; Yang *et al.*, 2021, 2024) to include uncoupled torsional and minor axis deformations using Vlasov's theory of thin-walled structures (Vlasov, 1961). Bebiano et al (Bebiano *et al.*, 2017) used generalized beam theory (GBT) to extend this solution to include cross-sectional deformation modes, and compared their predictions to a shell finite solution, highlighting its accuracy at a fraction of the computational cost. Detailed finite element models for high speed railway viaducts have typically focused on track wheel interaction (Knothe and Grassie, 1993; Lou, 2007; Song *et al.*, 2003; Xia and Zhang, 2005; Yang and Yau, 1997; Zhang *et al.*, 2016), although previous research (Frýba, 1972; Yang and Yau, 1997) has indicated that a moving load model is sufficient to predict viaduct response, while track wheel interaction is essential to analyze rolling stock behavior.

Finite element modeling remains prohibitively complex for routine design of HSR viaducts, but there is little guidance in design codes regarding applicable simplified analysis methods. To the authors' knowledge, the only guidelines regarding analysis are in BS EN 1991-2:2003 ("EN 1991-2: Eurocode 1: Actions on structures - Part 2: Traffic loads on bridges", 1991) which recommends that only bending eigenmodes may be used if the first torsional frequency is greater than 1.2 times the first natural frequency. Torsional modes are to be included in the analysis if their frequencies are within 1.2 times the fundamental frequency. This implies a modal analysis-based solution approach. The supporting research regarding applicability of modal analysis and need for including torsional eigenforms is scarce. There are at least two practical concerns that motivate research in this area. The true boundary conditions of the viaduct, which are typically compressive supports on the bottom flange at bearing locations, differ from simply supported or fixed assumptions in analytical approaches. Secondly, eccentric loading due to the passage of a train on one track, while the other track is empty, may result in an amplified torsional response. Additionally, GBT solutions on HSR viaducts (Bebiano *et al.*, 2017) have shown that the cross-sections undergo local deformations, and the applicability of simple beam-element solutions that neglect these merits investigation.

This work presents eigenvalue analysis results for viaduct sections using a simplified analytical approach, a GBT solution implemented through the opensource platform GBTuL (Bebiano *et al.*, 2018) and a solid finite element (FE) model built using ABAQUS (Dassault Systèmes 2023), considering idealized (simply supported) and realistic (bearing type) boundary conditions. Also compared are the dynamic deformation time histories under a single representative Japanese rolling stock. The applicability of different analysis approaches to the high-speed moving load problem for box girder viaducts is thus investigated.

2. Methodology

2.1 Beam theoretic solutions

Consider a simply supported beam of length L, under a series of moving axle loads of magnitude p, as shown in Figure 1.

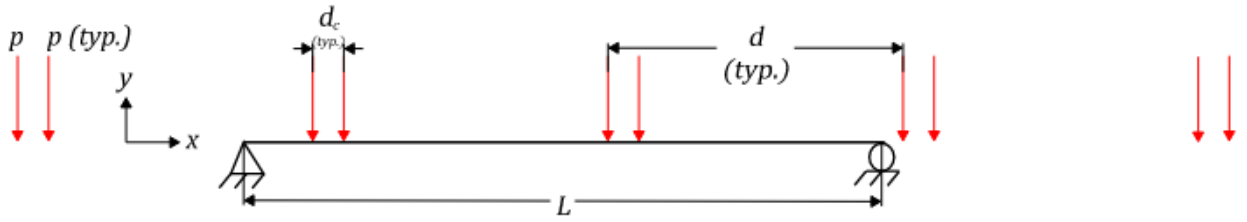

Figure 1: Simply supported beam under moving loads

The vertical deflection $u_y(x,t)$ of the beam, considering bending in the direction of loading only (i.e. about axis z) can be expressed as the product of time-dependent and location-dependent components:

$$u_y(x,t) = \sum_{n=1}^{\infty} y_n(t)\, sin(n\pi x/L) \tag{1}$$

Eq. 1 represents deflection $u_y(x,t)$ as a superposition of sinusoidal modes, n being the mode number. The time varying component $y_n(t)$ was derived in (Yang *et al.*, 1997, 2004) as:

$$y_n(t) = \frac{2pL^3}{EI_z\pi^4}[P_n(t) + P_n(t - t_c)] \tag{2}$$

where $t_c = d_c / v$ is the time lag between the two sets of axle loads moving at velocity v (see Fig. 1) and

$$P_n(t) = f(\omega_{yn}, \Omega_n, c_n, v, L) \tag{3}$$

Here the n^{th} natural frequency of the beam is $\omega_{yn} = \frac{n^2\pi^2}{L^2}\sqrt{EI_z/m}$ (E being modulus of elasticity, I_z moment of inertia about axis z, and m mass per unit length); excitation frequency is $\Omega_n = n\pi v/L$ and c_n is viscous damping coefficient. The function f is not repeated here for sake of brevity, and can be found in (Yang *et al.*, 1997)

Considering first mode effects only, resonance occurs when $sin(\omega_{y1} d/v) = 0$ which is useful to predict resonant speeds as a function of car length and girder properties.

Torsional and minor axis bending components are introduced in the formulation, based on Vlasov's theory for thin walled structures (Vlasov 1961;Xu et al. 2023; Yang et al. 2021, 2024). Vertical deflection is uncoupled from lateral and torsional displacements and can be calculated using Eqs. 1 through 3. Similar to Eq. 1, lateral and torsional displacements are expressed as a summation of sinusoidal modes, each broken up into two functions, one varying with time, and the other along length:

$$u_z(x,t) = \sum_{n=1}^{\infty} z_n(t)\, sin(n\pi x/L) \tag{4}$$

$$u_\theta(x,t) = \sum_{n=1}^{\infty} \theta_n(t)\, sin(n\pi x/L) \tag{5}$$

Similar to Eq. 2, the lateral and torsional deformations can be expressed as the summation of responses due to each set of axle loads at time lag t_c.

$$z_n(t) = Q_n(t) + Q_n(t - t_c) \tag{6}$$

$$\theta_n(t) = R_n(t) + R_n(t - t_c) \tag{7}$$

Response quantities Q_n and R_n can be expressed as:

$$Q_n(t) = g_1(\omega_{zn}, \omega_{\theta n}, \Omega_n, c_n, v, L) \tag{8}$$

$$P_n(t) = g_2(\omega_{zn}, \omega_{\theta n}, \Omega_n, c_n, v, L) \tag{9}$$

The functions g_1 and g_2 can be found in (Vlasov, 1961; Yang *et al.*, 2021). Eq. 8 and Eq. 9 indicate that the lateral and torsional responses are coupled through the frequencies $\omega_{zn}$and $\omega_{\theta n}$. These uncoupled frequencies can be defined as:

$$\omega_{zn} = \frac{n^2\pi^2}{L^2}\sqrt{EI_y/m} \tag{10}$$

$$\omega_{\theta n}^2 = \frac{EI_w(n\pi)^4 + GJ(n\pi L)^2}{m(\eta^2 + r^2)L^4} \tag{11}$$

where J and I_w are the torsion and warping constants respectively, G is shear modulus, η is distance of shear center from centroid, and r is polar radius of gyration. The coupled lateral torsional frequencies are:

$$\omega_{n^-}^2 = \frac{\left(\omega_{zn}^2 + \omega_{\theta n}^2\right) - \sqrt{\left(\omega_{zn}^2 - \omega_{\theta n}^2\right)^2 + 4\alpha\omega_{zn}^2\omega_{\theta n}^2}}{2(1-\alpha)} \tag{12}$$

$$\omega_{n^+}^2 = \frac{\left(\omega_{zn}^2 + \omega_{\theta n}^2\right) + \sqrt{\left(\omega_{zn}^2 - \omega_{\theta n}^2\right)^2 + 4\alpha\omega_{zn}^2\omega_{\theta n}^2}}{2(1-\alpha)} \tag{13}$$

These represent the low and high lateral torsional frequencies, with $\alpha = \frac{\eta^2}{\eta^2+r^2}$.

The solutions presented till this point require only the overall cross-sectional properties (I_y, I_z, J and I_w) irrespective of the actual shape. Generalized beam theory extends these solutions to

incorporate local cross-sectional modes such as distortion and local bending (Bebiano *et al.*, 2017, 2018), by accounting for coordinate s along the centerline of the cross-section, in addition to x coordinate along the length of viaduct. The solution is again expressed as a product of two responses; the first of these is the cross-sectional deformation, and the second is the time and length variant deformation:

$$u_y(x,s,t) = \sum_{k=1}^{N_d} \sum_{j=1}^{N_v} v_k(s)\varphi_{kj}(x)\varsigma_j(x,t) \tag{14}$$

$$u_z(x,s,t) = \sum_{k=1}^{N_d} \sum_{j=1}^{N_v} w_k(s)\varphi_{kj}(x)\varsigma_j(x,t) \tag{15}$$

considering N_d cross-sectional and N_v vibrational modes, where $v_k(s)$ and $w_k(s)$ are the vertical and horizontal displacements at location s for GBT mode k, and φ_{kj} is the modal contribution of the k^{th} GBT mode to the j^{th} vibrational mode.

Finding the cross-sectional GBT modes can be a challenging task but is conveniently conducted using the open-source program GBTUL (Bebiano *et al.*, 2018). The scope of this paper is limited to finding these cross-sectional modes and their contribution to global response using GBTUL.

2.2 Viaduct details

The details of the analyzed viaduct section are provided in Fig. 2. The bridge considered is a 40 m span viaduct inspired by the cross-sections in (Dai *et al.*, 2016). The cross-section is analyzed to study the impact of true boundary conditions on mode shapes and dynamic response.

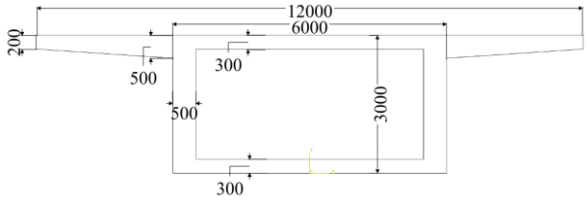

Figure 2: Analyzed cross-section (all dimensions are in mm)

2.3 Solid finite element modeling

A finite element (FE) model was built using ABAQUS (Dassault Systèmes 2023) to analyze the effect of boundary conditions on mode shapes and dynamic response of the viaduct, and the applicability of beam theory analytic solutions. Element types and mesh details are shown in Fig. 3. Eight noded solid 3D elements with reduced integration (C3D8R) are used because they were computationally tractable and precluded any kinematic assumptions of shell theory. Each element of the cross-section (i.e. flanges and webs) were discretized into a minimum of two finite elements.

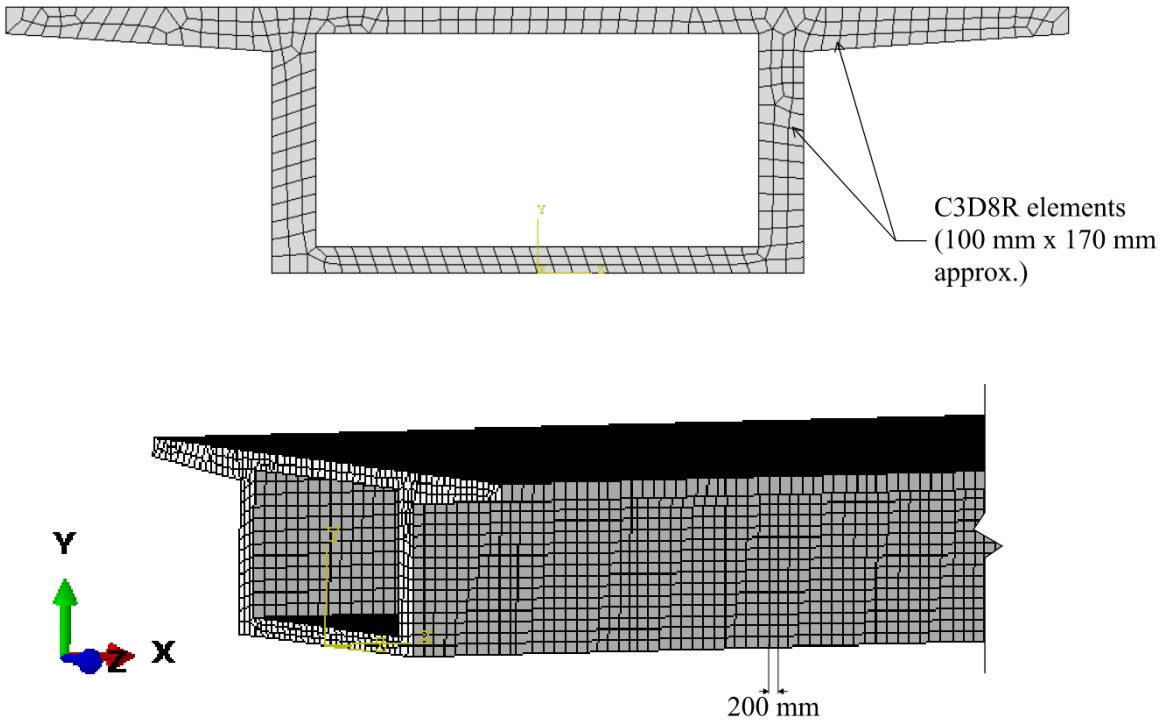

Figure 3: Solid FE model mesh and element details

Two sets of boundary conditions were considered, as shown in Fig. 4. In Case I, all nodes along the cross-section at the ends of the viaduct are restrained in vertical and lateral directions, and axially released. An axial restraint is provided along the bottom flange at mid-length to prevent rigid body displacement while allowing the cross-section to warp freely at the ends. The boundary condition is thus pinned, warping-free with torsional fixity.

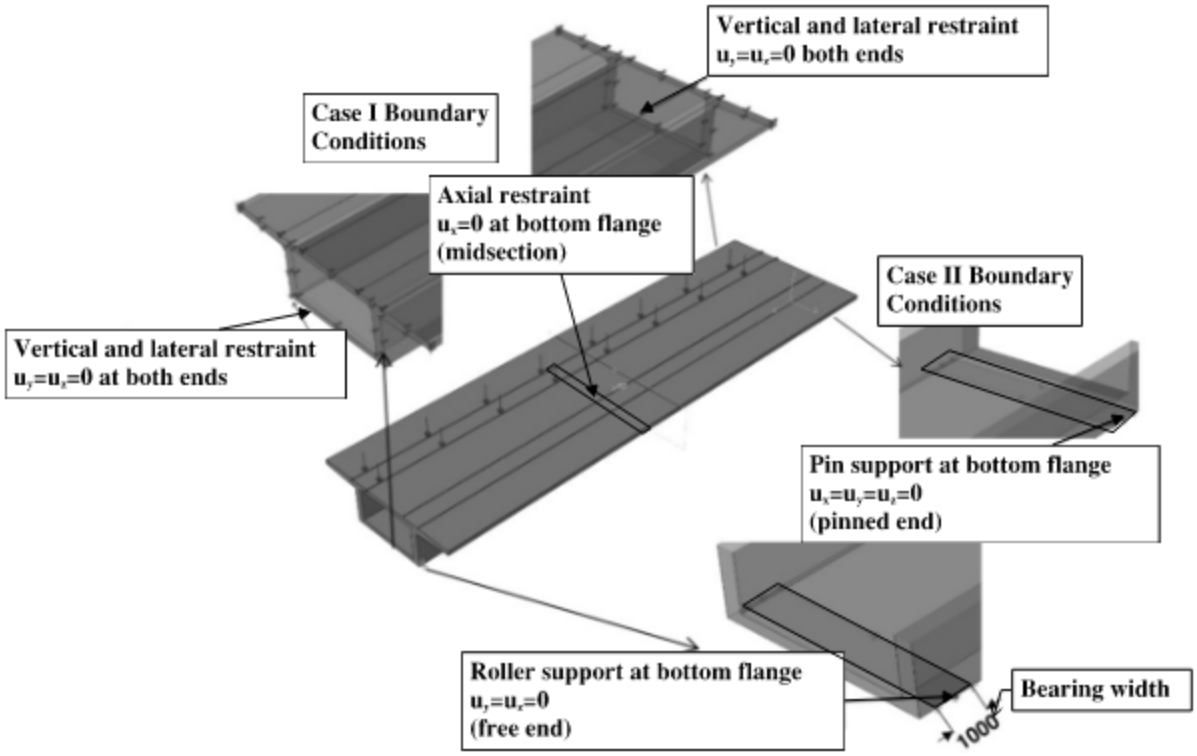

Figure 4: Assumed boundary conditions in the FE model

The second set of boundary conditions are intended to reflect a more practical scenario of bearing supports that are pinned at one end and rollers at the other (Case II in Fig. 4). A bearing width of 1000 mm is assumed over which the vertical and lateral degrees of freedom are restrained at both ends, and the axial degrees of freedom are restrained at one end. Similar to real bridge bearings, these restraints are applied only on the bottom flange of the viaduct.

Dynamic analysis with moving loads is conducted on the FE model to preclude the complexities of train-wheel-track interaction. The moving loads are applied as wheel pressure using custom user defined loading through FORTRAN. A linear dynamic explicit solution approach is adopted with output reported at time increments of 1e-4, and a Rayleigh mass proportional damping coefficient of $\alpha = 0.5$ corresponding to the modal damping of 2% critical assumed in the analytical solution. Only a single type of rolling stock – Japanese E5 train specified in (UIC (International Union of Railways), 2023), with p = 260 kN (for two axles), d_c = 5.7 m, and d = 23.7 m (see Fig. 1), with 10 cars (i.e. 10 couplets of point loads) is considered in the analysis. The case of a single train running on one track is considered, which introduces eccentricity due to its off-center location.

3. Results and discussions

3.1 Mode shapes and natural frequencies

Eigenvalues and mode shapes of the cross-section are predicted using GBT and the finite element model and listed in Fig. 5. These solutions assume simply support boundary conditions. This preliminary analysis includes only the self-weight of the viaduct. Eurocode BS EN 1991-2:2003 ("EN 1991-2: Eurocode 1: Actions on structures - Part 2: Traffic loads on bridges", 1991) recommends including "permanent actions" while predicting the natural frequencies, which would

imply inclusion of the permanent components of superimposed dead loads. For example, the study in (Bebiano *et al.*, 2017) included ballast, track and handrail masses in the analysis. The absence of this additional mass should be kept in mind while considering the results reported here.

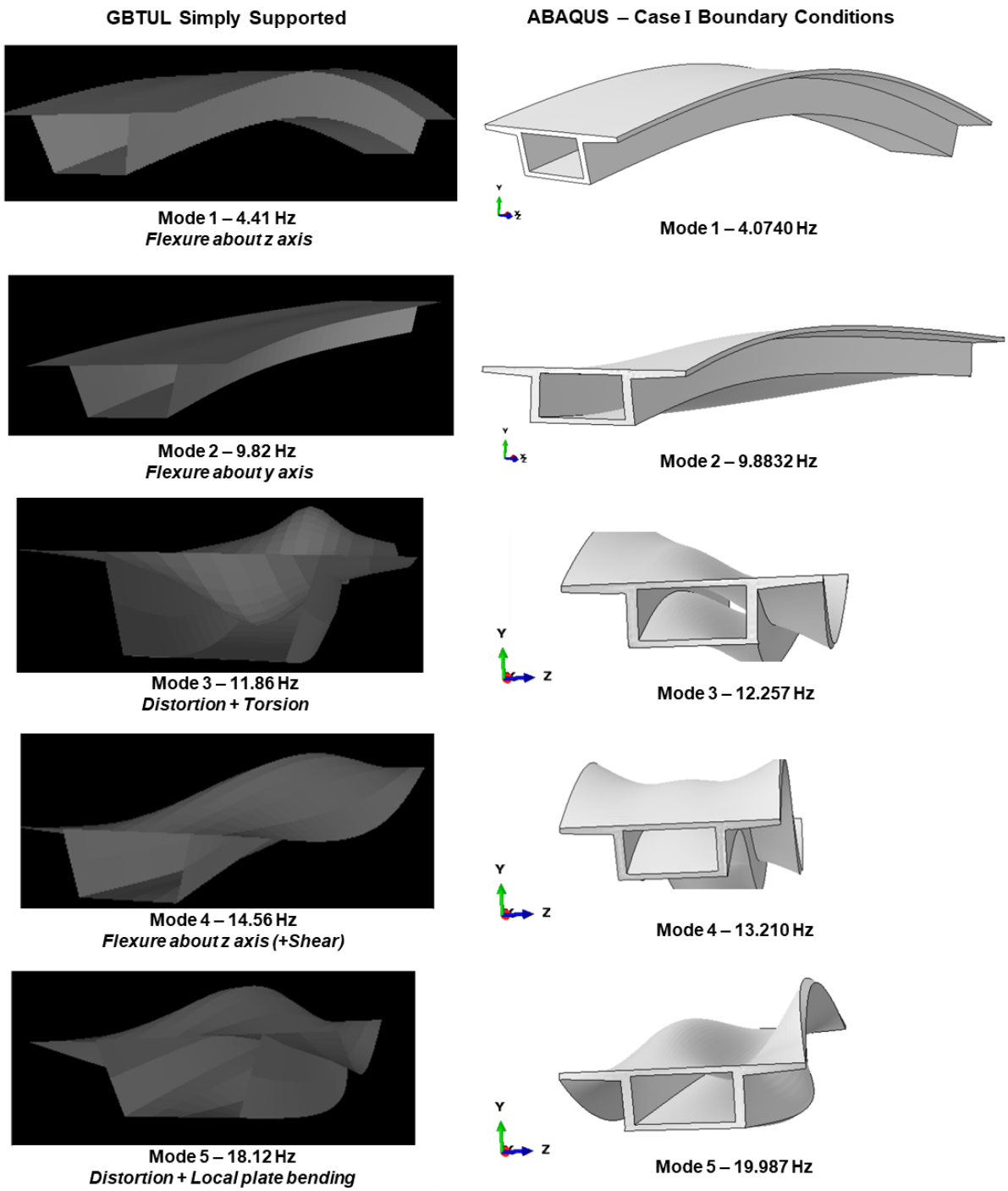

Figure 5: GBT and FE mode shapes for 40 m span cross-section, assuming simply supported boundary conditions

Fig. 5 indicates that GBT predicted frequencies and mode shapes are close to FE predictions, and torsional frequencies are well above 1.2 times the first natural bending frequency. These are also

broadly consistent with flexural (f_s), lateral (f_y), torsional (f_θ), and coupled torsional – lateral ($f_{z\theta^+}, f_{z\theta^-}$) eigenfrequencies analytically predicted using Eqs. 10 – 13 and listed in Table 1.

Table 1: Eigenfrequency values from analytical model. Frequency values are in Hz

Mode no.	f_y	f_z	f_θ	$f_{z\theta^+}$	$f_{z\theta^-}$
1	4	11	14	15	11
2	17	46	29	47	29

For the bearing type support (Case II Boundary Conditions as described in Fig. 4), the mode shapes and frequencies (listed in Fig. 6) are different from predictions that assumed Case I boundary conditions. The second mode shifts from lateral flexure (Case I boundary condition) to (what appears to be) a lateral torsional mode, presumably because the realistic bearing supports do not torsionally restrain the ends, which the analytically assumed boundary conditions do. Further, this eigenfrequency is much closer to 1.2 times the first natural frequency, but still larger. It is conjectured (without analysis) that the inclusion of permanent superimposed dead loads would potentially lower the vertical eigenfrequency without affecting the torsional mode. Finally, Case II boundary conditions result in a smaller clear span for the viaduct compared to Case I, which increases the flexural natural frequencies.

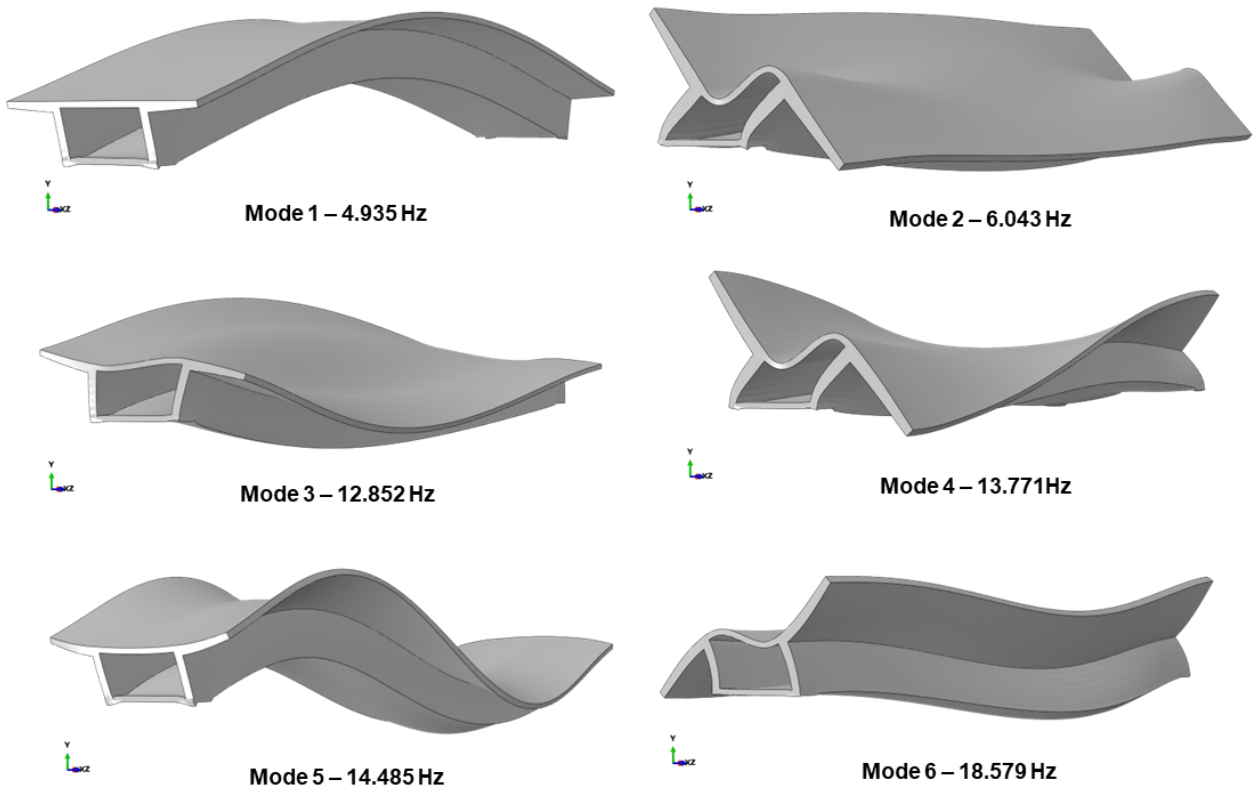

Figure 6: FE mode shapes and frequencies for bearing type boundary conditions

3.2 Deflection time histories

The dynamic response of a single train moving along the viaduct is analysed for a range of train speeds from 200 kmph to 350 kmph, using both analytical and FE models (both BCs). The flexural deflections at two representative speeds of 200 kmph and 300 kmph are shown in Fig. 7. The reported FE deflection is the average of values at all nodes on the outer boundary of the midspan cross-section.

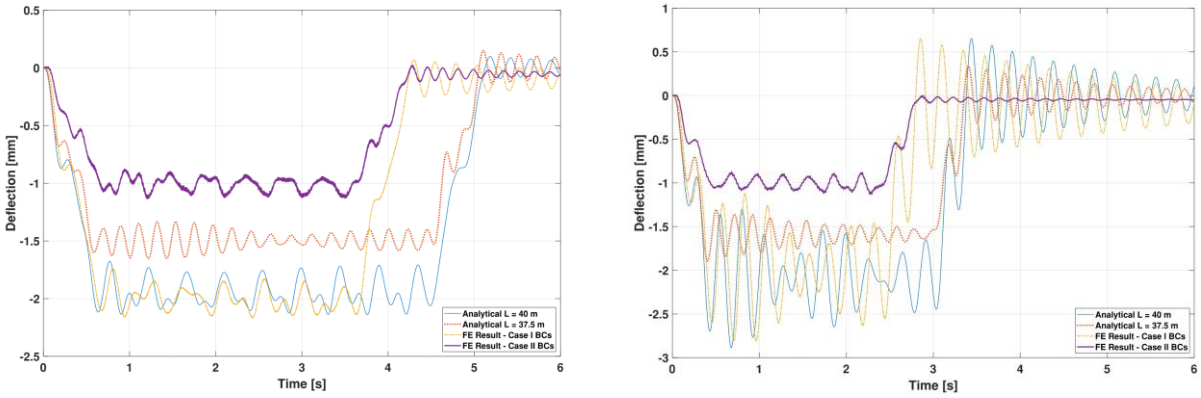

(a) Speed 200 kmph (b) Speed 300 kmph

Figure 7: Vertical deflection at viaduct midspan using analytical and FE solutions

The analytically predicted deflections are agreeable with FE results for Case I boundary conditions. For the bearing type boundary conditions, FE predictions are significantly smaller than the analytically predicted values assuming viaduct length as the clear span between the edges of bearing supports (i.e. 37.5 m). The likely cause of this is the moment fixity generated by the Case II bearing support due to the assumed width of 1000 mm. In reality, this moment fixity will not exist if bearing restraints are compression-only. This effect may be investigated further by modelling a single line of bearing support on the bottom flange instead of a finite width, or by using compressive contact modelling instead of pinned restraints.

3.3 Analytical prediction of resonant speeds

As discussed earlier, the dynamic interaction of bridge and train depends on girder properties, train speed and car length. Previous studies (Yang *et al.*, 1997) have proposed a speed parameter that predicts resonance by considering first mode response only, given as:

$$S_r = \frac{\pi v}{L\omega_1} = \frac{d}{2iL} \tag{15}$$

Given the car length (d) of a train and span of the bridge (L), the resonant speeds can be predicted as multiples of d/L. This is employed in this study ($d = 25m,\ L = 40m$) to identify the resonant speeds of the system. As shown in Fig. 8, the deflection peaks at speed parameter of around $\frac{d}{2iL} = 25 * \frac{2}{40} = 0.31$ which corresponds to a speed of 382 kmph. Additional peaks occur at fractions of this value, for example at speed parameters of 0.156 and 0.104 corresponding to train speeds of 191 kmph and 127 kmph, at which increased response amplifications are observed.

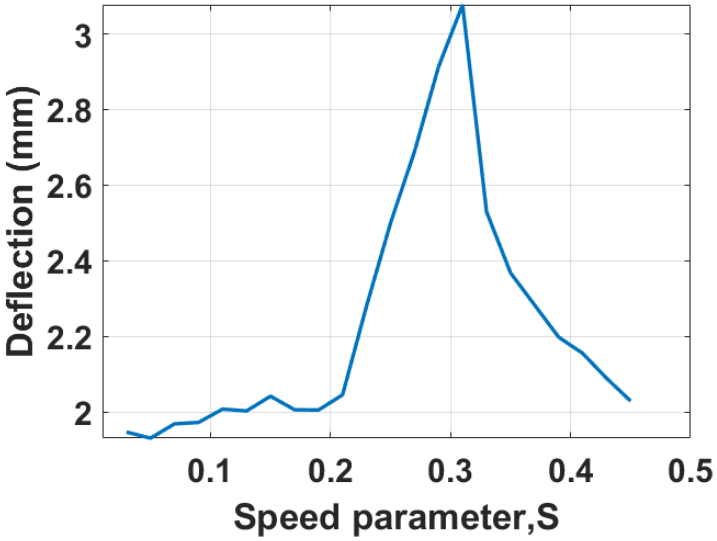

Figure 8: Speed parameter curve for E5 rolling stock and 40 m span simply supported viaduct (Fig. 2)

4. Conclusions

Although high speed railway viaducts require dynamic analysis at the design stage, there is little guidance in design standards regarding approaches to predict their dynamic response. The only provision currently available is in BS EN 1991-2:2003 which states that torsional eigenforms are to be excluded if the first natural torsional frequency is greater than 1.2 times the first natural frequency, but the research basis for this is unclear. Motivated by this gap, this paper presented four different approaches to solve the dynamic analysis problem – modal analysis including and excluding torsional eigenforms, a generalized beam theory solution implemented using the open-source application GBTUL(Bebiano *et al.*, 2018) and a solid finite element (FE) model. The FE analysis used moving loads without modelling wheel-track-girder interaction for simplicity, based on previous literature suggesting that this does not significantly alter viaduct response. The FE solution further included a realistic bearing type boundary condition to investigate its effects on the eigen analysis results.

Results indicate that GBT mode shapes and frequencies are close to the FE predictions in case of simply supported boundary conditions with torsional restraints, and for the cross-section analyzed here, the torsional frequency is beyond the prescribed limit. The lateral and torsional modes change significantly when the boundary conditions are altered to a realistic bearing-type support, possibly because this removes the torsional restraint applied on the entire cross-section. The change in boundary conditions appears to have lesser impact on the vertical flexural frequencies, potentially supporting the hypothesis that they are uncoupled from lateral and torsional modes. Although torsional frequencies approach the first natural frequency due to the modified boundary conditions, they remain outside the prescribed limits and will potentially be even further apart if permanent superimposed masses are added in the analysis, which is not done here.

Dynamic analyses conducted on the example cross-section using a single real train indicate that the simplified modal analysis solution excluding torsional eigenforms reasonably predict

deflection time histories and resonant speeds. Further analysis on other cross-sections and rolling stock is required to generalize this conclusion, particularly with sections where the first torsional eigenfrequency is close to the first natural frequency of the beam, or where local or distortional modes are dominant.

Acknowledgments
This work was financially supported by grant NHSRCL, HSRIC/VIADUCT/2022-23/003 from the High-Speed Railway Innovation Center of India. Their support is gratefully acknowledged.

References

Bebiano, R., Calçada, R., Camotim, D. and Silvestre, N. (2017), "Dynamic analysis of high-speed railway bridge decks using generalised beam theory", *Thin-Walled Structures*, Elsevier, Vol. 114, pp. 22–31, doi: 10.1016/J.TWS.2017.01.027.

Bebiano, R., Camotim, D. and Gonçalves, R. (2018), "GBTul 2.0 − A second-generation code for the GBT-based buckling and vibration analysis of thin-walled members", *Thin-Walled Structures*, Elsevier, Vol. 124, pp. 235–257, doi: 10.1016/J.TWS.2017.12.002.

Corp., D.S.S. (2023), "ABAQUS Software", Providence, RI, USA.

Dai, G., Su, M. and Chen, Y.F. (2016), "Design and construction of simple beam bridges for high-speed rails in China: standardization and industrialization", *The Baltic Journal of Road and Bridge Engineering*, Vol. 11 No. 4, pp. 274–282.

"EN 1991-2: Eurocode 1: Actions on structures - Part 2: Traffic loads on bridges". (1991), .

Frýba, L. (1972), *Vibration of Solids and Structures under Moving Loads*, Springer Netherlands.

Knothe, K.L. and Grassie, S.L. (1993), "Modelling of Railway Track and Vehicle/Track Interaction at High Frequencies", *Vehicle System Dynamics*, Taylor & Francis, Vol. 22 No. 3–4, pp. 209–262.

Lou, P. (2007), "Finite element analysis for train–track–bridge interaction system", *Archive of Applied Mechanics*, Vol. 77 No. 10, pp. 707–728.

Song, M.-K., Noh, H.-C. and Choi, C.-K. (2003), "A new three-dimensional finite element analysis model of high-speed train–bridge interactions", *Engineering Structures*, Vol. 25 No. 13, pp. 1611–1626.

"The Fortran Programming Language — Fortran Programming Language". (n.d.). , available at: https://fortran-lang.org/ (accessed 10 January 2026).

Timoshenko, S.P. (1922), "CV. On the forced vibrations of bridges", *The London, Edinburgh, and Dublin Philosophical Magazine and Journal of Science*, Informa UK Limited, Vol. 43 No. 257, pp. 1018–1019.

UIC (International Union of Railways). (2023), "Atlas, High-Speed Rail", UIC, Paris, France.

Vlasov, V.Z. (1961), *Thin-Walled Elastic Beams*, National Science Foundation, Washington, D.C.

Xia, H. and Zhang, N. (2005), "Dynamic analysis of railway bridge under high-speed trains", *Computers & Structures*, Vol. 83 No. 23, pp. 1891–1901.

Xu, H., Liu, Y.H., Yang, M., Yang, D.S. and Yang, Y.B. (2023), "Scanning and separating vertical and torsional–flexural frequencies of thin-walled girder bridges by a single-axle test vehicle", *Thin-Walled Structures*, Vol. 182, p. 110266.

Yang, Y.B., Mo, X.Q., Shi, K., Gao, S.Y., Liu, N. and Han, Z.Z. (2024), "Effect of damping on torsional-flexural frequencies of monosymmetric thin-walled beams scanned by moving vehicles", *Thin-Walled Structures*, Vol. 198, p. 111633.

Yang, Y.B., Mo, X.Q., Shi, K., Wang, Z.-L., Xu, H. and Wu, Y.T. (2021), "Scanning torsional-flexural frequencies of thin-walled box girders with rough surface from vehicles' residual contact response: Theoretical study", *Thin-Walled Structures*, Vol. 169, p. 108332.

Yang, Y.-B. and Yau, J.-D. (1997), "Vehicle-bridge interaction element for dynamic analysis", *Journal of Structural Engineering*, American Society of Civil Engineers, Vol. 123 No. 11, pp. 1512–1518.

Yang, Y.-B., Yau, J.D. and Hsu, L.C. (1997), "Vibration of simple beams due to trains moving at high speeds", *Engineering Structures*, Vol. 19, pp. 936–944.

Yang, Y.B., Yau, J.D. and Wu, Y.S. (2004), *Vehicle–Bridge Interaction Dynamics*, World Scientific.

Zhang, N., Tian, Y. and Xia, H. (2016), "A Train-Bridge Dynamic Interaction Analysis Method and Its Experimental Validation", *Engineering*, Vol. 2 No. 4, pp. 528–536.